Hindawi
Journal of Nanomaterials
Volume 2021, Article ID 6683040, 9 pages
https://doi.org/10.1155/2021/6683040

Research Article

Luminescence of Femtosecond Laser-Processed ZnSe Crystal

Igor Dmitruk,[1,2] **Nataliya Berezovska**,[1] **Volodymyr Degoda**,[1] **Yevhen Hrabovskyi**,[1] **Roman Kolodka**,[1] **Galyna Podust**,[1] **Oleksandr Stanovyi**,[1] **and Ivan Blonskyi**[2]

[1]*Faculty of Physics, Taras Shevchenko National University of Kyiv, Kyiv 01601, Ukraine*
[2]*Department of Photon Processes, Institute of Physics, NAS of Ukraine, Kyiv 03028, Ukraine*

Correspondence should be addressed to Nataliya Berezovska; n_berezovska@univ.kiev.ua

Received 29 November 2020; Revised 22 March 2021; Accepted 27 March 2021; Published 17 April 2021

Academic Editor: Hassan Karimi-Maleh

The ZnSe single crystal treatment in air environment with linearly polarized Ti/sapphire femtosecond (fs)laser pulses of the energy density of around 0.04-0.05 J/cm^2 with central wavelength of 800 nm and the pulse duration of 140 fs at a repetition rate of 1 kHz generates the laser-induced periodic surface structures (LIPSSs). The setup with a cylindrical quartz lens at normal incidence allowed processing a relatively large area of the ZnSe sample in one pass of the laser beam. Morphology analysis of LIPSS by scanning electron microscopy (SEM) and image processing reveals the existence of two periods of around 200.0 nm and 630.0 nm simultaneously. All LIPSSs demonstrate the orientation perpendicular to the laser beam polarization. The possible nature of LIPSS formation on ZnSe single crystal is caused by the synergetic influence of the interference mechanism involving surface plasmon polaritons and hydrodynamic effects of surface morphology modification. The fs-laser-induced changes of carrier concentrations in ZnSe specify obtained periods of high spatial frequency LIPSS. The influence of femtosecond laser processing on luminescent properties of ZnSe single crystal has been studied by an analysis of the photoluminescence (PL) and X-ray luminescence (XRL) spectra of laser-treated and untreated areas in the visible region of spectrum at room and low temperatures. The PL spectra and XRL spectra, as well as temperature dependencies of XRL spectra or thermally stimulated luminescence curves, demonstrate a good correlation for untreated and fs-laser-treated ZnSe surfaces. Specific PL bands related to the extended structural defects do not appear for LIPSS at the ZnSe sample under an excitation of 337 nm (3.68 eV). The Relative intensities and position of separate components of observed luminescence bands after ultrashort laser treatment do not change significantly. Thus, the structural perfection of the ZnSe single crystal surface is preserved.

1. Introduction

The physical and chemical properties of wide band gap semiconductor zinc selenide (ZnSe) are still of interest due to its promising applications for high-performance optoelectronic devices. ZnSe with the band gap energy of about 2.7 eV at 300 K is a perspective material for light-emitting diodes (LED) [1–3], photodetectors [4], field emitters, elements of solar cells [5, 6], and other areas. ZnSe is also used as γ-radiation semiconductor detectors [7] and X-ray detectors that operate in a wide temperature range up to 130°C [8].

In recent decades, along with traditional techniques aimed at the synthesis of high-quality crystalline materials, in particular semiconductor single crystals with low concentrations of uncontrolled impurities, the rapidly developed methods of nanotechnology provide new promising materials of nanoscale dimensionality with unique properties for different fields of life—from medicine and electronics to the improvement of environment. For instance, new nanocomposites could use green technology during their synthesis [9]. The nanotechnology actively involves designed nanoparticles for medical applications as delivery agents of drugs, for light or the constituent elements of biosensors [10], and for the elements in optoelectronic devices [11], photoelectrochemical cells [12], etc. The methods of surface modification of the materials with the aim of forming nanoscale surface structures are also actively elaborated.

In the comprehensive review [13], it is noted that nanostructured ZnSe belongs to the most popular optoelectronic materials due to the novel properties and its unique applications that become another promising area in ZnSe research.

There are few studies devoted to the surface modification of ZnSe under the influence of femtosecond (fs) laser pulses that provide submicron surface ripples at the edges of ablation craters or on the whole ablation area in the case of the sample moving under a certain laser power [14–17]. Some authors obtained periodic structures with similar periods but with different orientations relative to the laser polarization. After the fs-laser irradiation of ZnSe single crystal, Jia et al. [14] obtained specific regular nanogratings of a period of about 180 nm parallel to the polarization of the incident laser beam. Ma et al. [15] observed laser-induced periodic structures with the period of about 160 nm aligned perpendicular to the laser beam polarization. The Authors interpreted the formation of such nanogratings by the interference between the incident light of 800 nm wavelength and the surface scattered wave induced by the incident laser radiation. Nevertheless, the nature of such laser-induced nanostructures is still under discussion.

Processing of the ZnSe surface with powerful fs-laser pulses realizes some effects that are perspective for application in optoelectronics. For instance, a rapid growth method of nanowires of 1–3 μm long and 50–150 nm in diameter in liquid has been demonstrated for potential applications in microscopic optoelectronics [18]. Luo et al. demonstrated the fabrication of hexagonal ZnSe nanoparticles on the surface of submicron ripples using fs-laser pulses in air [19]. Wang et al. [20] obtained spherical-shaped wurtzite ZnSe nanoparticles by ultrahigh ablation pressure at the local area due to the sudden injection of high energy leading to solid-solid transition. They stated that the average size of nanoparticles can be varied from ~16 nm to ~22 nm in diameter by means of the fs-laser fluence control.

Usually, impurities and native defects fundamentally affect electronic, optical, and magnetic properties of both single crystals and nanosized solid-state materials [21]. In some cases, native defects can demonstrate either a donor or an acceptor character and form complexes with dopant impurities. Thus, in this contribution, we study the influence of the fs-laser processing on luminescent properties of ZnSe at room and low temperatures to elucidate possible changes in impurity-defect quality of ZnSe single crystals after fs-laser treatment.

2. Experimental Details

An undoped ZnSe single crystal of 2 mm thickness with maximum resistivity ($\rho \geq 10^{12}\,\Omega \cdot \mathrm{cm}$) has been used for femtosecond laser texturing. ZnSe crystal grown by the Czochralski method from a prepurified batch is characterized with a minimum concentration of impurities. The ultrashort laser pulses obtained from an amplified Ti:sapphire femtosecond laser system (Coherent Inc.) have been used for laser treatment. In our study, the linearly polarized high-intensity femtosecond laser pulses with a wavelength of 800 nm and the pulse duration of 140 fs at a repetition rate of 1 kHz are focused on the sample surface by a cylindrical quartz lens with 100.0 mm focal length at normal incidence. This setup allows processing a relatively large area of the sample in one pass of the laser beam. The distance between the focusing lens and the ZnSe sample provides a certain value of laser radiation power density. During the laser processing, a vertically standing sample stage moves at a velocity of 1 mm/s. The minimum laser beam spot area on the sample surface was $3.0 \times 10^{-2}\,\mathrm{cm}^2$. The fs-laser processing is carried out at normal temperature and pressure.

The morphology of ZnSe surfaces before and after the ultrashort laser treatment has been analysed using a scanning electron microscope (SEM) AURA 100 (SERON Technology Inc.).

The experimental studies of photoluminescence (PL) and X-ray luminescence (XRL) have been carried out at room and liquid nitrogen temperatures. The ZnSe sample was placed in the cryostat for measurements at the temperature of liquid nitrogen. The X-ray excitation has been performed by the integral radiation of the X-ray tube BCV8 (Cu, 20 kV, 25 mA) through the beryllium window of the cryostat in the perpendicular direction to the sample surface. All X-ray irradiation was absorbed within the sample. The distance from the anode of the X-ray tube to the sample was 120 mm. The luminescence has been registered through two channels: integrally and spectrally. The integral glow of the sample was focused (an optical filter was used if necessary) by a quartz lens on a photocathode of the photoelectric multiplier PMT-106. The luminescence radiation passing through another quartz window of the cryostat was registered by the monochromator MDR-2 with quartz condensers and recorded by the photoelectric multiplier PMT-106. All spectra were adjusted taking into account the spectral sensitivity of the recording system. The spectra were corrected to the spectral radiation density while converting the spectra from the wavelength scale (nm) to the quanta energy scale (eV). The PL spectra have been measured with the setup based on a single-grating spectrometer MDR-3 with the inverse linear dispersion of 2.6 nm/mm under an excitation of semiconductor laser $\lambda_{ex} = 406$ nm ($E_{ex} = 3.05$ eV) and pulsed nitrogen laser $\lambda_{ex} = 337$ nm ($E_{ex} = 3.68$ eV).

3. Results and Discussion

3.1. Peculiarities of LIPSS Formation on the ZnSe Surface under Ultrashort Laser Pulses. The treatment of the ZnSe single crystal surface with the linear polarized fs-laser pulses with a wavelength of 800 nm leads to the formation of the laser-induced periodic surface structures (LIPSSs) with a period much shorter than the irradiation wavelength and an orientation perpendicular to the laser beam polarization (see Figures 1(a) and 1(b)). We treated two areas of the ZnSe sample with fs-laser pulses of 800 nm wavelength. Surface N1 was processed by the radiation with a pulse energy density of $0.038\,\mathrm{J/cm}^2$ at the repetition rate of 1 kHz and the efficient number of laser pulses $N = 400$, and surface N2 by the radiation with $0.05\,\mathrm{J/cm}^2$ at the repetition rate of 1 kHz and the efficient number of laser pulses $N = 300$. The surface coating with LIPSSs is rather homogeneous. We actually do not observe the products of the ablation process, which usually takes place under laser processing. We applied the lower-fluence multipulse regime that realized the laser processing below the fs-laser ablation threshold. As known, the ablation

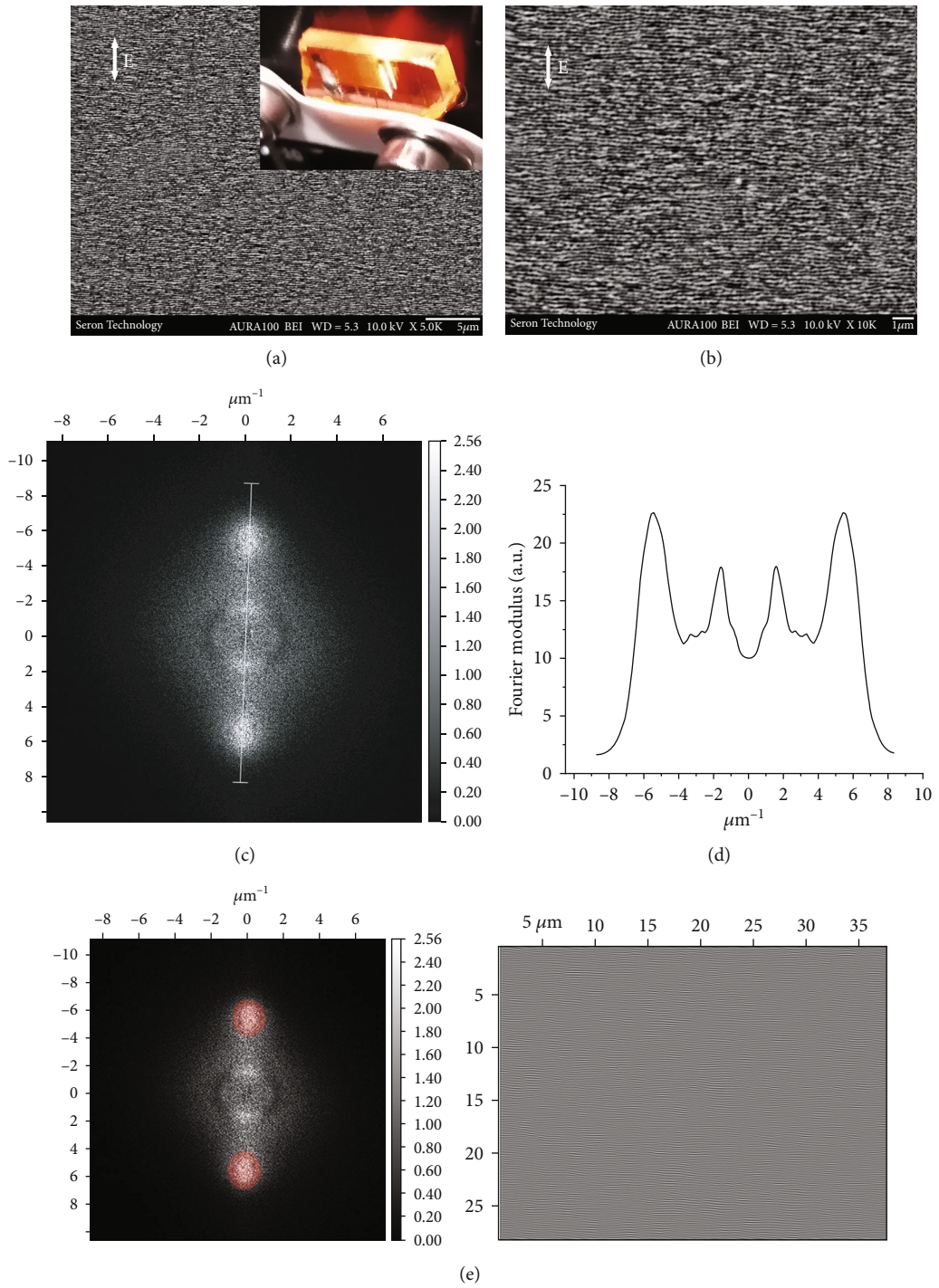

Figure 1: Continued.

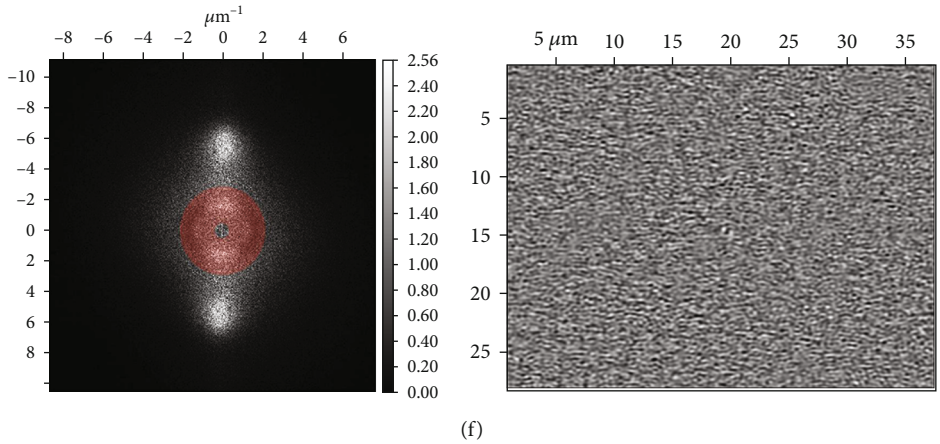

Figure 1: SEM images of ZnSe laser-treated surface N2 with different magnification (a, b), 2D Fourier transform of a SEM image (a) of ZnSe surface N2 (c), Fourier transform profile along the line at 2D Fourier transform (d), and two kinds of the inverse transform of 2D Fourier transform presented at (c) (e, f). Red circles at 2D Fourier transform images indicate the areas that have been taken for the inverse transform. The inset at (a) presents the process of fs-laser treatment of ZnSe single crystal.

threshold for ZnSe is about $0.7\,\mathrm{J/cm^2}$ [22]. The LIPSS parameters obtained in our experiments correlate with the data of the previous studies [14, 15, 17, 23].

The periodicity of obtained LIPSSs has been evaluated quantitatively by 2D Fourier transform of ZnSe SEM images. 2D Fourier transform has been performed using Gwyddion 2.56 software. LIPSS periods vary from 182 to 214 nm depending on a slight change in processing parameters for surfaces N1 and N2. These spatial periods are known as high spatial frequency LIPSS (HSFL).

2D Fourier transform of ZnSe SEM images demonstrates an existence of additional periodicity, namely, the presence of LIPSS with period of 629 or 635 nm depending on a slight change in laser processing parameters for surfaces N1 and N2. The direction of ripples in this LIPSS is perpendicular to the laser beam polarization. This kind of LIPSS is commonly referred to as low spatial frequency LIPSS (LSFL). We performed the inverse transform of 2D Fourier transform to evaluate the periods of relevant quasigratings. This procedure is presented in Figures 1(e) and 1(f). The red circles on 2D Fourier transform images indicate the areas that have been taken for calculation and as a result give corresponding quasigrating shown in the picture nearby. The periods of reversely obtained quasigratings match the periods evaluated from real SEM image of LIPSS at the ZnSe surface.

The recent reviews [24–26] emphasize that the study of the nature of LIPSS formation in different materials remains a current topic for many research groups in this field. The most accepted phenomenon that explains the formation of LSFL is the interference of the incident laser radiation with surface electromagnetic waves including generated surface plasmon polaritons (SPPs) at the surface roughness of the initial sample that is followed by a spatial and periodical modulation of energy deposition. The first ultrashort pulses can also produce surface roughness that may facilitate the excitation of SPPs. This mechanism is actual for the plasmonically active materials, e.g., metals, and explains the formation of the LSFL with period values close to the laser wavelength. In the case of the initially plasmonically nonactive materials, such as semiconductors and dielectrics, the involvement of the SPP mechanism may be reasonable when the critical electron density is exceeded, and such materials turn into a metallic state [27]. Earlier, we have observed the formation of LSFL on the surface of metal-semiconductor composite sample Au/(n-Si) [28]. The periods of LSFLs formed at Au or Si surfaces under certain laser power densities had close orders of magnitude. Bonse et al. [29] demonstrated that LSFLs at the silicon surface are formed involving generated SPP, but they mentioned that such phenomenon was actual for relatively narrow fluence range where the laser-induced carrier concentration increased up to the order of 10^{21}–$10^{22}\,\mathrm{cm^{-3}}$. Tsibidis et al. [30] emphasize the synergetic approach which takes into account hydrodynamic effects besides the mechanism involving SPP. This approach explains satisfactorily the LSFL period of about 630 nm obtained in our experiments for laser-treated ZnSe single crystal.

The periods Λ of HSFL in transparent material usually follow closely the empirical formula $\Lambda \simeq (\lambda/2n)$, where n is the refractive index of an untreated material and λ is the wavelength of the incident laser beam. One of the first models that tried to explain mentioned values of fine ripple periods has been presented by Buividas et al. in 2011 [31]. Thus, the HSFL was formed from plasma nanospheres localized in the bulk of the irradiated material at the prebreakdown conditions, i.e., when the electron plasma density did not reach critical value. Moreover, they noticed that the HSFL period was not dependent on the pulse energy. In our case, we observe slight dependence of HSFL on pulse energy density. The authors [14, 23, 29] point to the transient changes in material properties under ultrashort laser irradiation. Therefore, for laser-induced ZnSe, the complex refractive index $n^*(\lambda)$ is considered as a function of the carrier density in the conduction band. Based on the Drude model, modified femtosecond laser-excited refractive index n^* for ZnSe is lower than that for untreated material. Thus, Wang et al. [23] obtained for the laser-treated ZnSe the HSFL period of 200 ± 10 nm. The values of HSFL periods obtained in our

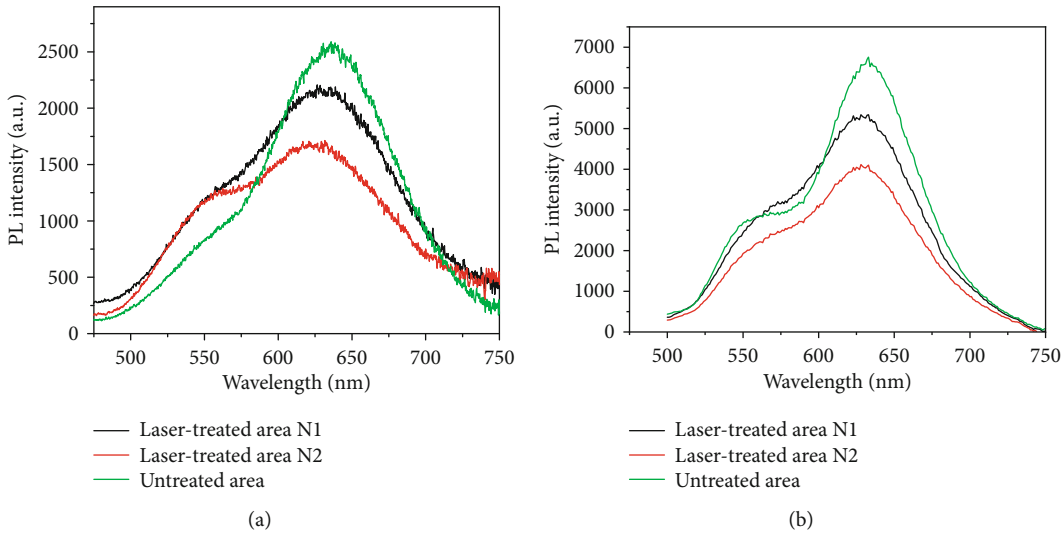

Figure 2: PL spectra of different areas of the ZnSe sample at 300 (a) and 77 K (b) under the laser excitation at 406 nm wavelength: green line indicates the untreated ZnSe surface, black line indicates fs-laser-treated surface N1, and red line indicates fs-laser-treated surface N2.

experiments are in good accordance with results from the mentioned paper.

3.2. Impact of fs-Laser Processing on Luminescent Properties of ZnSe Single Crystal. The next step intends to study the luminescent properties of a ZnSe semiconductor after fs-laser treatment. It is known that the XRL and PL spectra for a high-resistance ZnSe semiconductor at nitrogen and room temperatures in the visible and near IR region have the main emission bands with the maxima in the range of 460–480 nm (2.69–2.58 eV), around 550 nm (2.25 eV), 630 nm (1.97 eV), and 970 nm (1.28 eV). The nature of the mentioned luminescence bands has been considered in numerous papers [32–35]. The most acceptable explanations state that the bands in "blue" region are determined by excitons bound at various impurities and defects and the recombination of donor-acceptor pairs. The impurity-defect complexes define the "green" band of the spectrum. The band with a maximum at about 630 nm is caused by the crystal complex center containing a Zn vacancy. The luminescence band of about 970 nm is determined by the complex center with the Cu impurity or the Se vacancy.

In our experiments, we elucidate the influence of the fs-laser treatment on X-ray luminescence and photoluminescence properties of ZnSe single crystal in the visible region of the spectrum.

At room temperature, the PL spectra of the laser-treated ZnSe surfaces differ from the PL of the untreated area. PL studies have been performed with an excitation at a wavelength of 406 nm. It can be noted that the PL spectra of all considered surfaces differ from each other. The PL spectrum of the untreated surface has a pronounced peak at around 630 nm (see Figure 2). For both laser-treated areas, this band demonstrates a slight shift but in different directions of the wavelengths. Thus, the wide emission band at about 630 nm is probably not elementary. The full width at half maximum (FWHM) of the band at around 630 nm increases with growing temperature due to the increase in the vibrational level population of the excited electron states of the luminescence centers. The complex nature of this wide band is caused by both electronic and hole recombination mechanisms of luminescence realized at corresponding recombination centers [36]. The authors of contributions [36–38] suppose that in the vicinity of a dipole center, either a free electron or a free hole can be localized. Moreover, this band has been observed in the spectra of phosphorescence and thermally stimulated luminescence (TSL) that confirm the recombination nature of this radiation [36]. The Relative intensity of this band for an untreated area is considerably higher than the one of the laser-treated areas at lower temperature (see Figure 2(b)).

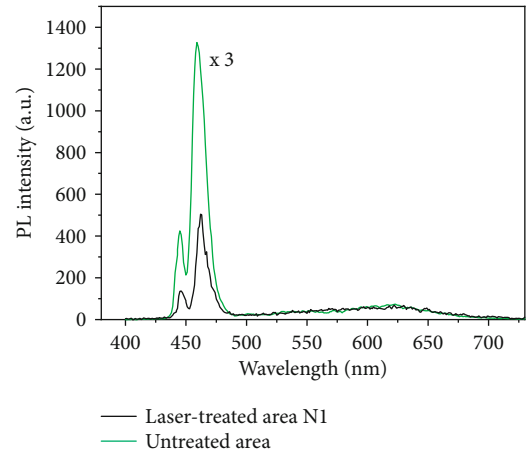

Figure 3: PL spectra of the ZnSe sample at 77 K under the laser excitation at 337 nm wavelength: green line indicates the untreated ZnSe surface and black line indicates fs-laser-treated surface N1.

Wide band around 550 nm is determined by intrinsic point defects (Zn interstitials and Zn vacancies) with oxygen or other impurities (Cu, Al) [34, 35]. In the PL spectra of laser-treated ZnSe surfaces, a small shift of the band in the

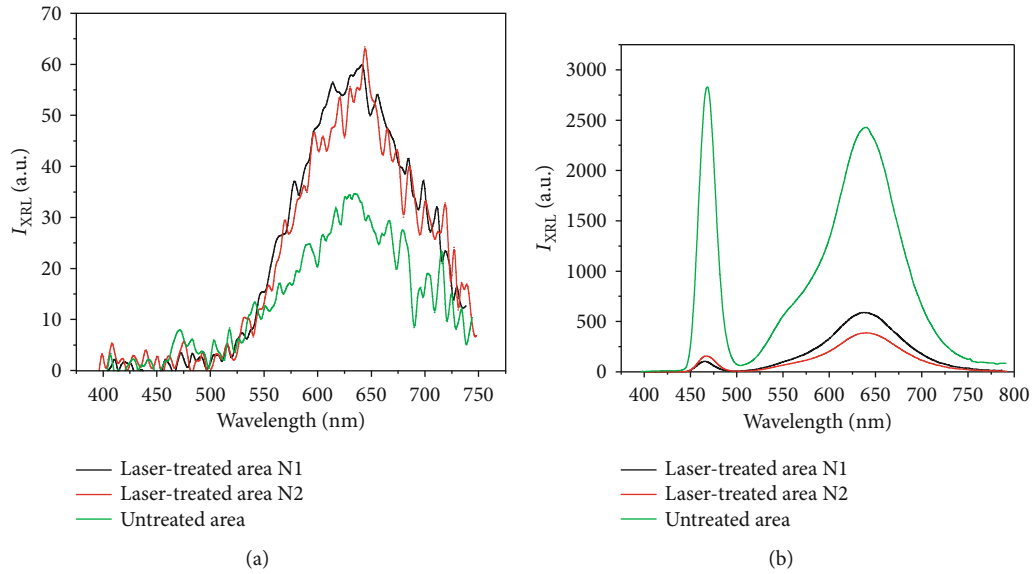

Figure 4: XRL spectra of untreated and fs-laser-treated areas of the ZnSe sample at 300 K (a) and 85 K (b).

region around 550 nm to long-wavelength region is observed at the liquid nitrogen temperature.

We also studied near-band-edge emission and emission related to the impurities or structural defects at liquid nitrogen temperature. The PL spectra of untreated and laser-treated areas of the ZnSe sample under an excitation of 337 nm (3.68 eV) are presented in Figure 3. The PL band at 445.2 nm (2.78 eV) attributed to the excitonic recombination at Zn vacancy-related acceptors [39] and wide PL band at about 461.3 nm (2.687 eV) reveal noticeably higher intensity for the untreated area of the ZnSe sample in comparison to the fs-laser-treated area whereas the bands in the region from 500 to 700 nm are of the same order of magnitude (see Figure 3). For one of the fs-laser-treated areas of the ZnSe sample, the PL band at about 462.3 nm (2.68 eV) demonstrates the nonelementary character under the laser excitation at 337 nm. ZnSe near-band-edge emission spectra under the excitation at 337 nm (3.68 eV) evidently manifested complex structure of the wide PL band in the region of 460–480 nm mainly due to the recombination of donor-acceptor pairs in ZnSe single crystal. The redistribution of the relative intensity of the PL band components for untreated and fs-laser-treated areas has been observed. We should also note that PL bands related to the extended structural defects do not appear for the created LIPSS at the ZnSe sample. We can only notice hardly observable shoulder of 463.7 nm at the slope of the band. It may indicate that the high structural perfection of ZnSe single crystal is not affected significantly during fs-laser processing, while some structural defects could be produced and/or not removed by the mechanical polishing [39].

The tendencies in XRL data coincided with the influence of powerful ultrashort laser processing on PL spectra. It should be noted that the higher intensity of the complex broad band around 630 nm at X-ray excitation in comparison with the one at an excitation at 406 nm is caused by different conditions of luminescence recording (Figure 4).

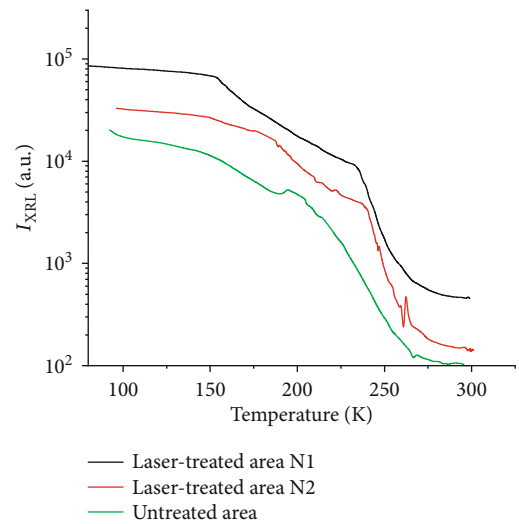

Figure 5: Temperature dependence of XRL spectra of untreated and fs-laser-treated areas of the ZnSe sample.

Temperature dependence of XRL spectra reveals that the intensities of luminescence bands attributed to different areas of the ZnSe sample remain almost unchanged up to 150 K. Then, intensities of all corresponding bands begin to decline rapidly starting from the temperature of around 250 K (see Figure 5).

The attenuation of phosphorescence and TSL curves reveals similar behaviour for the fs-laser-treated and as-grown ZnSe sample (see Figure 6). Meanwhile, it should be noted that the peak ratio has the tendency to change for fs-laser-treated surfaces, and the low-temperature peak for an untreated surface demonstrates higher intensity.

The fs-laser processing reveals slight decrease in the charge-carrier lifetime and a decay of luminescence, but it is not crucial and indicates almost the same number of the

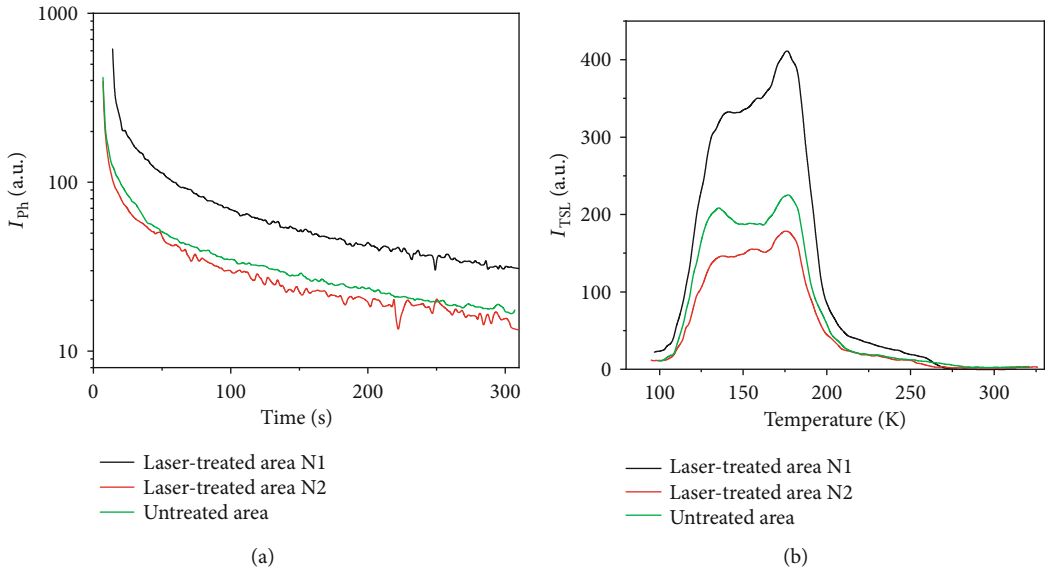

Figure 6: Phosphorescence decay at 85 K (a) and TSL curves for untreated and fs-laser-treated areas of the ZnSe sample (b).

recharged emission centers after the laser processing. The decrease in the relative intensity of PL and XRL of the fs-laser-treated surfaces of the ZnSe sample is similar to the effect observed during mechanical polishing of ZnSe samples [35].

Nevertheless, high quality of luminescence of the laser-treated surface confirms its structure perfection. It opens up the way for reuse of ZnSe single crystal for analytical purposes.

4. Conclusions

The processing of ZnSe single crystal with powerful femtosecond laser induces the formation of LIPSSs on a relatively large ablation area with satisfactory uniformity of surface filling. Analysis of the morphology and 2D Fourier transform of the obtained SEM images of the fs-laser-treated ZnSe surface reveal at the processed surface the quasigratings of two periods: around 200 nm and 630 nm. The periods of LIPSSs slightly grow with the increase in the laser fluence. The possible nature of obtained LIPSSs for fs-laser-treated ZnSe can be attributed to the interference of incident radiation with the surface plasmon polaritons and the influence of hydrodynamic effects during ripple formation. The fs-laser-induced changes of carrier density in the ZnSe semiconductor to a large extent specify the period of obtained HSFL.

The changes in luminescent properties of ZnSe single crystal under femtosecond laser irradiation have been revealed by means of the PL and XRL measurements. Some features observed in luminescence spectra of treated areas such as decreased relative intensities of some PL bands and appearance of additional bands are similar to the effects noticed during mechanical polishing of ZnSe samples. The PL and XRL spectra demonstrate a good correlation in spite of their difference in relative intensities and position of separate components of the observed luminescence bands. Thus, the high structural perfection of ZnSe single crystal is not affected crucially during the femtosecond laser treatment that could be meaningful for further prospective applications of such ZnSe surfaces.

Data Availability

(1) The data on PL and XRL spectra used to support the findings of this study are available from the corresponding author upon request. (2) Previously reported data on the nature of the emission band at about 630 nm are used to support this study and are available at appropriate doi:10.1016/j.physb.2015.02.021 which is cited at a relevant place within the text as a reference [36], doi:10.15407/fm24.02.206 which is cited at a relevant place within the text as a reference [37], and doi:10.1016/j.ijleo.2019.164139 which is cited at a relevant place within the text as a reference [38].

Additional Points

Highlights. (i) The treatment of ZnSe single crystal with femtosecond laser radiation induces the formation of LIPSSs of two periods: around 200 nm and 630 nm. (ii) The changes of carrier density in ZnSe under femtosecond laser essentially determine the nature of ripple formation. (iii) After femtosecond laser treatment, the PL and XRL spectra of ZnSe single crystal demonstrate a good correlation.

Conflicts of Interest

The authors declare that they have no conflicts of interest.

Acknowledgments

The authors acknowledge the funding from the Ministry of Education and Science of Ukraine (Project No. 19BF051-04, State reg. no. 0119U100300) and appreciate the technical support of the Femtosecond Laser Center for Collective Use of NAS of Ukraine.

References

[1] V. K. Sharma, B. Guzelturk, T. Erdem, Y. Kelestemur, and H. V. Demir, "Tunable white-light-emitting Mn-doped ZnSe nanocrystals," *ACS Applied Materials & Interfaces*, vol. 6, no. 5, pp. 3654–3660, 2014.

[2] W. Ji, P. Jing, W. Xu et al., "High color purity ZnSe/ZnS core/-shell quantum dot based blue light emitting diodes with an inverted device structure," *Applied Physics Letters*, vol. 103, no. 5, article 053106, 2013.

[3] K. Ou, L. Bai, M. Huang, L. Yi, X. Duan, and S. Wang, "Effect of preparation parameters on deep-blue light-emitting diodes based on nanostructured ZnSe/ZnS multilayer films," *ACS Omega*, vol. 5, no. 38, pp. 24567–24573, 2020.

[4] V. Naval, C. Smith, V. Ryzhikov, S. Naydenov, F. Alves, and G. Karunasiri, "Zinc selenide-based Schottky barrier detectors for ultraviolet-A and ultraviolet-B detection," *Advances in OptoElectronics*, vol. 2010, Article ID 619571, 5 pages, 2010.

[5] Y. Chen, X. Mei, X. Liu et al., "Solution-processed CdTe thin-film solar cells using ZnSe nanocrystal as a buffer layer," *Applied Sciences*, vol. 8, no. 7, article 1195, 2018.

[6] X. Zhang, J. Mao, Z. Shao et al., "Efficient photovoltaic devices based on p-ZnSe/n-CdS core–shell heterojunctions with high open-circuit voltage," *Journal of Materials Chemistry C*, vol. 5, no. 8, pp. 2107–2113, 2017.

[7] A. O. Sofiienko and V. Y. Degoda, "X-ray induced conductivity of ZnSe sensors at high temperatures," *Radiation Measurements*, vol. 47, no. 1, pp. 27–29, 2012.

[8] M. S. Brodyn, V. Y. Degoda, A. O. Sofiienko, B. V. Kozhushko, and V. T. Vesna, "Monocrystalline ZnSe as an ionising radiation detector operated over a wide temperature range," *Radiation Measurements*, vol. 65, pp. 36–44, 2014.

[9] Y. Orooji, R. Mohassel, O. Amiri, A. Sobhani, and M. Salavati-Niasari, "Gd_2ZnMnO_6/ZnO nanocomposites: green sol-gel auto-combustion synthesis, characterization and photocatalytic degradation of different dye pollutants in water," *Journal of Alloys and Compounds*, vol. 835, article 155240, 2020.

[10] H. Karimi-Maleh, M. Alizadeh, Y. Orooji et al., "Guanine-based DNA biosensor amplified with Pt/SWCNTs nanocomposite as analytical tool for nanomolar determination of daunorubicin as an anticancer drug: a docking/experimental investigation," *Industrial & Engineering Chemistry Research*, vol. 60, no. 2, pp. 816–823, 2021.

[11] J. Ning, J. Liu, Y. Levi-Kalisman, A. I. Frenkel, and U. Banin, "Controlling anisotropic growth of colloidal ZnSe nanostructures," *Journal of the American Chemical Society*, vol. 140, no. 44, pp. 14627–14637, 2018.

[12] F. Huang, J. Ning, W. Xiong et al., "Atomic sulfur passivation improves the photoelectrochemical performance of ZnSe nanorods," *Nanomaterials*, vol. 10, no. 6, article 1081, 2020.

[13] Q. Zhang, H. Li, Y. Ma, and T. Zhai, "ZnSe nanostructures: synthesis, properties and applications," *Progress in Materials Science*, vol. 83, pp. 472–535, 2016.

[14] T. Q. Jia, H. X. Chen, M. Huang et al., "Formation of nanogratings on the surface of a ZnSe crystal irradiated by femtosecond laser pulses," *Physical Review B*, vol. 72, no. 12, article 125429, 2005.

[15] H. L. Ma, Y. Guo, M. J. Zhong, and R. X. Li, "Femtosecond pulse laser-induced self-organized nanogratings on the surface of a ZnSe crystal," *Applied Physics A*, vol. 89, no. 3, pp. 707–709, 2007.

[16] L. Wang, Q.-D. Chen, R. Yang et al., "Rapid production of large-area deep sub-wavelength hybrid structures by femtosecond laser light-field tailoring," *Applied Physics Letters*, vol. 104, no. 3, article 031904, 2014.

[17] Y. Xiao, G. Deng, G. Feng et al., "Femtosecond laser induced nano-meter size surface structures on ZnSe film," *AIP Advances*, vol. 9, no. 1, article 015106, 2019.

[18] T. Jia, M. Baba, M. Huang et al., "Femtosecond laser-induced ZnSe nanowires on the surface of a ZnSe wafer in water," *Solid State Communications*, vol. 141, no. 11, pp. 635–638, 2007.

[19] C. W. Luo, H. I. Wang, L. W. Liao, C. S. Yang, and T. Kobayashi, "Preparation of ZnSe nanoparticles with femtosecond laser," in *2011 International Quantum Electronics Conference (IQEC) and Conference on Lasers and Electro-Optics (CLEO) Pacific Rim incorporating the Australasian Conference on Optics, Lasers and Spectroscopy and the Australian Conference on Optical Fibre Technology*, pp. 1993-1994, Sydney, NSW, Australia, August-September 2011.

[20] H. I. Wang, W. T. Tang, L. W. Liao et al., "Femtosecond laser-induced formation of wurtzite phase ZnSe nanoparticles in air," *Journal of Nanomaterials*, vol. 2012, Article ID 278364, 6 pages, 2012.

[21] M. Isshiki and J. Wang, "Wide-bandgap II-VI semiconductors: growth and properties," in *Springer Handbook of Electronic and Photonic Materials*, S. Kasap and P. Capper, Eds., pp. 365–383, Springer, Cham, 2017.

[22] X. Wang, T. Jia, X. Li et al., "Ablation and ultrafast dynamics of zinc selenide under femtosecond laser irradiation," *Chinese Optics Letters*, vol. 3, no. 10, pp. 615–617, 2005.

[23] S. Wang, G. Feng, and S. Zhou, "Microsized structures assisted nanostructure formation on ZnSe wafer by femtosecond laser irradiation," *Applied Physics Letters*, vol. 105, no. 25, article 253110, 2014.

[24] R. Buividas, M. Mikutis, and S. Juodkazis, "Surface and bulk structuring of materials by ripples with long and short laser pulses: recent advances," *Progress in Quantum Electronics*, vol. 38, no. 3, pp. 119–156, 2014.

[25] C. Florian, S. V. Kirner, J. Krüger, and J. Bonse, "Surface functionalization by laser-induced periodic surface structures," *Journal of Laser Applications*, vol. 32, no. 2, article 022063, 2020.

[26] J. Bonse and S. Gräf, "Maxwell meets Marangoni—a review of theories on laser-induced periodic surface structures," *Laser & Photonics Reviews*, vol. 14, no. 10, article 2000215, 2020.

[27] M. Huang, F. Zhao, Y. Cheng, N. Xu, and Z. Xu, "Origin of laser-induced near-subwavelength ripples: interference between surface plasmons and incident laser," *ACS Nano*, vol. 3, no. 12, pp. 4062–4070, 2009.

[28] N. Berezovska, I. Dmitruk, A. Kalyuzhnyy, A. Dmytruk, and I. Blonskyi, "Self-organized structuring of the surface of a metal–semiconductor composite by femtosecond laser processing," *Ukrainian Journal of Physics*, vol. 63, no. 5, pp. 406–412, 2018.

[29] J. Bonse, A. Rosenfeld, and J. Krüger, "On the role of surface plasmon polaritons in the formation of laser-induced periodic surface structures upon irradiation of silicon by femtosecond-laser pulses," *Journal of Applied Physics*, vol. 106, no. 10, article 104910, 2009.

[30] G. D. Tsibidis, M. Barberoglou, P. A. Loukakos, E. Stratakis, and C. Fotakis, "Dynamics of ripple formation on silicon surfaces by ultrashort laser pulses in subablation conditions," *Physical Review B*, vol. 86, no. 11, article 115316, 2012.

[31] R. Buividas, L. Rosa, R. Šliupas et al., "Mechanism of fine ripple formation on surfaces of (semi) transparent materials via a half-wavelength cavity feedback," *Nanotechnology*, vol. 22, no. 5, article 055304, 2011.

[32] R. N. Bhargava, R. J. Seymour, B. J. Fitzpatrick, and S. P. Herko, "Donor-acceptor pair bands in ZnSe," *Physical Review B*, vol. 20, no. 6, pp. 2407–2419, 1979.

[33] V. Ryzhikov, B. Grinyov, S. Galkin, N. Starzhinskiy, and I. Rybalka, "Growing technology and luminescent characteristics of ZnSe doped crystals," *Journal of Crystal Growth*, vol. 364, pp. 111–117, 2013.

[34] A. A. Gladilin, N. N. Ilichev, V. P. Kalinushkin et al., "Study of the effect of doping with iron on the luminescence of zinc-selenide single crystals," *Semiconductors*, vol. 53, no. 1, pp. 1–8, 2019.

[35] I. Abbasov, M. Musayev, J. Huseynov et al., "Photoluminescence spectra of polycrystalline ZnSe in different experimental geometries," *Ukrainian Journal of Physical Optics*, vol. 21, no. 2, pp. 103–114, 2020.

[36] V. Y. Degoda, N. Y. Pavlova, G. P. Podust, and A. O. Sofiienko, "Spectral structure of the X-ray stimulated phosphorescence of monocrystalline ZnSe," *Physica B: Condensed Matter*, vol. 465, pp. 1–6, 2015.

[37] M. Alizadeh, V. Y. Degoda, B. V. Kozhushko, and N. Y. Pavlova, "Luminescence of dipole-centers in ZnSe crystals," *Functional Materials*, vol. 24, no. 2, pp. 206–211, 2017.

[38] M. S. Brodyn, V. Y. Degoda, N. Y. Pavlova et al., "The components of 630-nm band in ZnSe and their recombination mechanisms," *Optik*, vol. 208, article 164139, 2020.

[39] J. A. García, A. Remón, A. Zubiaga, V. Muñoz-Sanjosé, and C. Martinez-Tomás, "Photoluminescence study of ZnSe single crystals obtained by solid phase recrystallization under different pressure conditions. Effects of thermal treatment," *Physica Status Solidi (A)*, vol. 194, no. 1, pp. 338–348, 2002.